

## 基于柔性四羧酸的三个一维/二维/三维 Zn(II)/Co(II)配合物的晶体结构及荧光性质

刘露<sup>1</sup> 靳平宁<sup>2</sup> 杨杰<sup>3</sup> 宋立星<sup>1</sup> 赵博<sup>1</sup>  
李金科<sup>1</sup> 黄斌<sup>1</sup> 张裕平<sup>1</sup> 杨晓迅<sup>\*,1</sup>  
(<sup>1</sup>河南科技学院化学化工学院, 新乡 453003)  
(<sup>2</sup>新乡医学院基础医学院, 新乡 453003)  
(<sup>3</sup>安阳职业技术学院, 安阳 455008)

**摘要:** 通过水热/溶剂热合成的方法制备了3个Zn(II)/Co(II)配合物 $\{[Zn(H_2L)(H_2O)_3] \cdot H_2O \cdot 0.5H_4L\}_n$  (**1**)、 $\{[Co(L)_{0.5}(4,4'-bpy)] \cdot 0.5H_2O\}_n$  (**2**)和 $\{[Co(L)_{0.5}(pbmb)(H_2O)] \cdot H_2O\}_n$  (**3**)( $H_4L=5,5'$ -(hexane-1,6-diyl)-bis(oxy)diisophthalic acid,  $4,4'$ -bpy=4,4'-bipyridine, pbmb=1,1'-(1,3-propane)bis-(2-methylbenzimidazole))。结构分析表明配合物**1**为一维链结构。**2**为拓扑符号为 $(6^4 \cdot 7 \cdot 8)(6 \cdot 7^2)$ 的三重穿插网络结构。**3**是拓扑符号为 $(4 \cdot 6^2)(4^2 \cdot 6^2 \cdot 8^2)$ 的(3,4)-连接的二维网络结构。配合物**1**呈现出较好的荧光性质。

**关键词:** Zn(II); Co(II); 晶体结构; 拓扑; 荧光

中图分类号: O614.24<sup>+</sup>1; O614.81<sup>+</sup>2

文献标识码: A

文章编号: 1001-4861(2021)05-0921-08

DOI: 10.11862/CJIC.2021.101

### Structure and Fluorescence Properties of Three 1D/2D/3D Zn(II)/Co(II) Complexes Based on Flexible Tetracarboxylic Acid

LIU Lu<sup>1</sup> JIN Ping-Ning<sup>2</sup> YANG Jie<sup>3</sup> SONG Li-Xing<sup>1</sup> ZHAO Bo<sup>1</sup>  
LI Jin-Ke<sup>1</sup> HUANG Bin<sup>1</sup> ZHANG Yu-Ping<sup>1</sup> YANG Xiao-Xun<sup>\*,1</sup>

(<sup>1</sup>School of Chemistry and Chemical Engineering, Henan Institute of Science and Technology, Xinxiang, Henan 453003, China)

(<sup>2</sup>Department of Basic Medical Science, Xinxiang Medical University, Xinxiang, Henan 453000, China)

(<sup>3</sup>Anyang Vocational and Technical College, Anyang, Henan 455008, China)

**Abstract:** Three complexes, namely  $\{[Zn(H_2L)(H_2O)_3] \cdot H_2O \cdot 0.5H_4L\}_n$  (**1**),  $\{[Co(L)_{0.5}(4,4'-bpy)] \cdot 0.5H_2O\}_n$  (**2**) and  $\{[Co(L)_{0.5}(pbmb)(H_2O)] \cdot H_2O\}_n$  (**3**) ( $H_4L=5,5'$ -(hexane-1,6-diyl)-bis(oxy)diisophthalic acid,  $4,4'$ -bpy=4,4'-bipyridine, pbmb=1,1'-(1,3-propane)bis-(2-methylbenzimidazole)), have been prepared by solvo-/hydrothermal reactions. Complex **1** belongs to a 1D chain structure. Complex **2** presents a 3D 3-fold interpenetrating framework with the Schläfli symbol  $(6^4 \cdot 7 \cdot 8)(6 \cdot 7^2)$ . Complex **3** features a (3,4)-connected 2D network with the Schläfli symbol  $(4 \cdot 6^2)(4^2 \cdot 6^2 \cdot 8^2)$ . Complex **1** exhibited better fluorescence properties. CCDC: 1968748, **1**; 1968750, **2**; 1968751, **3**.

**Keywords:** Zn(II); Co(II); crystal structure; topology; fluorescence

收稿日期: 2020-10-16. 收修改稿日期: 2021-01-11.

河南科技学院高层次人才科研启动项目、河南科技学院标志性创新工程项目(No.2015BZ02)、创新团队培育工程项目(No.2018T02)、河南省高等学校重点科研项目(No.17A150027)和河南省科技攻关项目(No.212102210308)资助。

\*通信联系人。E-mail: liululu2012@126.com

Metal-organic frameworks, as a new kind of stable and tunable materials composing of organic bridging ligands and metal centers, have become very attractive candidates for gas storage, drug delivery, molecule separation, *etc*<sup>[1-5]</sup>. In order to fabricate useful metal-organic frameworks materials, the researchist have made sorts of theoretical predictions and adopt various methods to control the topological structure and geometry configuration. The organic ligands as building blocks play a major role in the design of the materials. We know many multidentate aromatic carboxylic acid ligands have been widespread employed to fabricate metal-organic frameworks materials<sup>[6-9]</sup>, because of their robustness and thermal stability<sup>[10]</sup>. Based on our previous widespread research on metal-organic frameworks materials, we predict that the ether-linked flexible tetracarboxylic acids ligand 5,5'-(hexane-1,6-diyl)-bis(oxy)diisophthalic acid (H<sub>4</sub>L) would be a splendid precursor for the construction of the ideal structures. Firstly, the H<sub>4</sub>L ligand can afford various coordination fashions by deprotonated to the corresponding species (H<sub>3</sub>L<sup>-</sup>, H<sub>2</sub>L<sup>2-</sup>, HL<sup>3-</sup>, and L<sup>4-</sup>). Secondly, the existence of the —(CH<sub>2</sub>)<sub>6</sub>— spacers and the two methoxy groups will cause the carboxyl groups to joint to metal ions in different directions, resulting in the formation of more possibilities of topologies. On the side, N-heterocyclic spacers as secondary coligand will also be a good approach that could forward structural diversity.

Hence, by introducing two N-donor coligands into the Zn(II)/Co(II)/H<sub>4</sub>L synthesis system, three complexes, formulated as {[Zn(H<sub>2</sub>L)(H<sub>2</sub>O)<sub>3</sub>]·H<sub>2</sub>O·0.5H<sub>4</sub>L}<sub>n</sub> (**1**), {[Co(L)<sub>0.5</sub>(4,4'-bpy)]·0.5H<sub>2</sub>O}<sub>n</sub> (**2**) and {[Co(L)<sub>0.5</sub>(pbmb)(H<sub>2</sub>O)]·H<sub>2</sub>O}<sub>n</sub> (**3**) (4,4'-bpy=4,4'-bipyridine, pbmb=1,1'-(1,3-propane)bis-(2-methylbenzimidazole)) were successfully acquired. The photoluminescent properties of complex **1** were also covered.

## 1 Experimental

### 1.1 Materials and methods

All reagents and solvents were commercially available except for pbmb, which was synthesized according to the literature<sup>[11]</sup>. FT-IR spectra were recorded on a FTIR-7600 spectrophotometer with KBr pellets in 400~

4 000 cm<sup>-1</sup> region. Elemental analyses (C, H and N) were carried out on a FLASH EA 1112 elemental analyzer. The fluorescence spectra for the samples were measured by a F7000 fluorescence spectrophotometer. The excitation slit and emission slit was 2.0 nm.

### 1.2 Synthesis of {[Zn(H<sub>2</sub>L)(H<sub>2</sub>O)<sub>3</sub>]·H<sub>2</sub>O·0.5H<sub>4</sub>L}<sub>n</sub> (**1**)

A mixture of Zn(NO<sub>3</sub>)<sub>2</sub>·6H<sub>2</sub>O (0.029 7 g, 0.1 mmol), H<sub>4</sub>L (0.022 3 g, 0.05 mmol), CH<sub>3</sub>CN (2 mL) and distilled H<sub>2</sub>O (6 mL) was placed in a 25 mL Teflon-lined stainless-steel container. The mixture was sealed and heated at 130 °C for three days. After the final mixture was gradually cooled to ambient temperature by a rate of 5 °C·h<sup>-1</sup>, the colourless crystals of **1** were acquired with a yield of 50% (based on Zn). Anal. Calcd. for C<sub>33</sub>H<sub>35</sub>O<sub>19</sub>Zn(%): C, 49.48; H, 4.40. Found(%): C, 49.45; H, 4.42. IR (KBr, cm<sup>-1</sup>): 3 444(w), 2 946(w), 1 619(m), 1 554(s), 1 459(m), 1 390(s), 1 322(m), 1 261(m), 1 135(m), 1 041(s), 995(w), 935(w), 779(s), 725(m).

### 1.3 Synthesis of {[Co(L)<sub>0.5</sub>(4,4'-bpy)]·0.5H<sub>2</sub>O}<sub>n</sub> (**2**)

A mixture of Co(NO<sub>3</sub>)<sub>2</sub>·6H<sub>2</sub>O (0.058 2 g, 0.2 mmol), H<sub>4</sub>L (0.044 6 g, 0.1 mmol), 4,4'-bpy (0.031 2 g, 0.2 mmol) and distilled H<sub>2</sub>O (15 mL) was heated at 120 °C for two days in a 25 mL Teflon-lined stainless-steel vessel. The purple crystals of **2** were obtained with a yield of 25% (based on Co). Anal. Calcd. for C<sub>21</sub>H<sub>18</sub>CoN<sub>2</sub>O<sub>5.5</sub>(%): C, 56.64; H, 4.07; N, 6.29. Found (%): C, 56.60; H, 4.05; N, 6.31. IR (KBr, cm<sup>-1</sup>): 3 338 (m), 3 072(vw), 2 942(s), 2 873(m), 2 356(w), 1 729(s), 1 668(s), 1 608(s), 1 558(s), 1 417(s), 1 386(s), 1 330 (s), 1 280(s), 1 216(s), 1 182(s), 1 120(s), 1 041(s), 889 (s), 815(vs), 771(vs), 736(s), 709(vs), 669(vs), 630(vs), 592(s), 568(s), 512(vs).

### 1.4 Synthesis of {[Co(L)<sub>0.5</sub>(pbmb)(H<sub>2</sub>O)]·H<sub>2</sub>O}<sub>n</sub> (**3**)

A mixture of Co(OAc)<sub>2</sub>·4H<sub>2</sub>O (0.049 8 g, 0.2 mmol), H<sub>4</sub>L (0.044 6 g, 0.1 mmol), pbmb (0.060 8 g, 0.2 mmol), NaOH (0.016 0 g, 0.4 mmol) and distilled H<sub>2</sub>O (8 mL) was heated at 120 °C for three days in a 25 mL Teflon-lined stainless-steel vessel. After the final mixture was gradually cooled to ambient temperature by a rate of 5 °C·h<sup>-1</sup>, the purple crystals of **3** were obtained with a yield of 41% (based on Co). Anal. Calcd. for C<sub>30</sub>H<sub>33</sub>CoN<sub>4</sub>O<sub>7</sub>(%): C, 58.06; H, 5.36; N,

9.02. Found(%): C, 58.09; H, 5.33; N, 9.04. IR (KBr,  $\text{cm}^{-1}$ ): 3 542(w), 3 451(w), 3 413(w), 2 946(w), 1 668(w), 1 558(vs), 1 459(vs), 1 386(vs), 1 288(w), 1 143(w), 1 033(vs), 892(w), 736(s).

### 1.5 Crystal structural determination

The crystal data of **1**~**3** were collected on a Rigaku Saturn 724 CCD diffractometer (Mo  $K\alpha$ ,  $\lambda = 0.071\ 073$  nm) at temperature of 293(2) K. Absorption corrections were applied by using multi-scan program. The data were modified for Lorentz and polarization effects. The

structures were solved by direct methods and refined with a full-matrix least-squares technique based on  $F^2$  with the SHELX-97 crystallographic software package<sup>[12]</sup> or OLEX2<sup>[13]</sup>. SQUEEZE was used in the crystal structure analysis of complex **2**. Crystallographic crystal data and structure processing parameters for **1**~**3** are summarized in Table 1. Selected bond lengths and bond angles of **1**~**3** are listed in Table 2.

CCDC: 1968748, **1**; 1968750, **2**; 1968751, **3**.

**Table 1** Crystallographic data and structure refinement details for complex **1**~**3**

Complex	<b>1</b>	<b>2</b>	<b>3</b>
Formula	$\text{C}_{33}\text{H}_{35}\text{O}_{19}\text{Zn}$	$\text{C}_{21}\text{H}_{18}\text{CoN}_2\text{O}_{5.5}$	$\text{C}_{30}\text{H}_{33}\text{CoN}_4\text{O}_7$
Formula weight	800.98	445.31	620.53
Crystal system	Triclinic	Monoclinic	Triclinic
Space group	$P\bar{1}$	$P2_1/c$	$P\bar{1}$
$a$ / nm	0.867 77(17)	0.844 56(17)	0.919 64(18)
$b$ / nm	1.051 2(2)	1.437 3(3)	1.193 5(2)
$c$ / nm	2.049 4(4)	1.777 6(5)	1.369 5(3)
$\alpha$ / ( $^\circ$ )	101.53(3)		85.40(3)
$\beta$ / ( $^\circ$ )	91.43(3)	107.42(3)	80.23(3)
$\gamma$ / ( $^\circ$ )	101.49(3)		76.39(3)
$V$ / $\text{nm}^3$	1.790 9(6)	2.058 8(8)	1.438 5(5)
$Z$	2	4	2
$D_c$ / ( $\text{g}\cdot\text{cm}^{-3}$ )	1.485	1.408	1.433
$\mu$ / $\text{mm}^{-1}$	0.768	0.867	0.651
$F(000)$	830	896	648
$\theta$ range / ( $^\circ$ )	2.02~25.50	2.40~25.49	1.51~27.88
GOF	1.052	0.993	0.993
$R_1$ [ $I > 2\sigma(I)$ ] <sup>a</sup>	0.098 4	0.098 1	0.047 0
$wR_2$ [ $I > 2\sigma(I)$ ] <sup>b</sup>	0.205 4	0.268 4	0.115 7

$$^a R_1 = \sum ||F_o| - |F_c|| / \sum |F_o|; ^b wR_2 = [\sum w(F_o^2 - F_c^2)^2 / \sum w(F_o^2)^2]^{1/2}.$$

**Table 2** Selected bond lengths (nm) and bond angles ( $^\circ$ ) for **1**~**3**

Complex <b>1</b>					
Zn1—O1	0.232 7(4)	Zn1—O2	0.206 2(4)	Zn1—O6	0.228 2(10)
Zn1—O7	0.198 4(5)	Zn1—O8	0.228 4(7)	Zn1—O9	0.195 0(4)
O2—Zn1—O1	58.89(16)	O2—Zn1—O8	83.2(2)	O6—Zn1—O1	89.5(2)
O7—Zn1—O1	84.04(17)	O2—Zn1—O6	85.2(3)	O7—Zn1—O2	142.92(18)
O9—Zn1—O7	108.83(18)	O9—Zn1—O2	107.97(17)	O9—Zn1—O1	166.02(17)
O7—Zn1—O8	93.6(3)	O9—Zn1—O8	88.1(2)	O7—Zn1—O6	96.5(3)
O6—Zn1—O8	168.3(3)	O8—Zn1—O1	85.6(2)	O9—Zn1—O6	94.2(2)
Complex <b>2</b>					
Co1—O1	0.238 2(6)	Co1—O2	0.202 5(6)	Co1—O3#1	0.199 7(6)
Co1—N1	0.207 2(6)	Co1—N2	0.210 8(6)		

Continued Table 2

N1—Co1—N2	95.5(2)	O2—Co1—N1	146.5(3)	N1—Co1—O1	96.5(2)
N2—Co1—O1	88.6(2)	O2—Co1—N2	105.3(3)	O2—Co1—O1	58.9(2)
O3#1—Co1—O1	157.6(2)	O3#1—Co1—N1	105.2(2)	O3#1—Co1—O2	98.9(2)
O3#1—Co1—N2	94.9(2)				
Complex 3					
Co1—O1	0.204 89(16)	Co1—O6	0.222 39(19)	Co1—N1	0.209 3(2)
Co1—N3	0.216 0(2)	Co1—O4#1	0.219 60(17)	Co1—O5#1	0.214 59(18)
O1—Co1—N1	97.19(8)	O1—Co1—N3	95.87(7)	N1—Co1—N3	90.50(8)
O1—Co1—O6	87.43(7)	N1—Co1—O6	89.43(8)	N3—Co1—O6	176.68(7)
O1—Co1—O4#1	153.49(7)	N1—Co1—O4#1	107.48(7)	N3—Co1—O4#1	93.53(8)
O5#1—Co1—N3	92.15(8)	O1—Co1—O5#1	94.54(7)	N1—Co1—O5#1	167.65(7)
O5#1—Co1—O4#1	60.32(6)	O4#1—Co1—O6	83.33(7)	O5#1—Co1—O6	87.23(8)

Symmetry codes: #1:  $x, -y+3/2, z-1/2$  for **2**; #1:  $x-1, y, z$  for **3**.

## 2 Results and discussion

### 2.1 Crystal structure of $\{[\text{Zn}(\text{H}_2\text{L})(\text{H}_2\text{O})_3] \cdot \text{H}_2\text{O} \cdot 0.5\text{H}_4\text{L}\}_n$ (**1**)

Crystallographic analysis reveals that **1** crystallizes in the triclinic system with  $P\bar{1}$  space group. As depicted in Fig. 1a, the asymmetric unit comprises one crystallographically independent Zn(II) ion, a  $\text{H}_2\text{L}^{2-}$  ligand, three coordinated water molecules, one lattice water molecule and half a dissociative  $\text{H}_4\text{L}$  ligand. Zn(II) ion is six-coordinated with coordination geometry of octahedron, which is completed by two oxygen atoms (O1 and O2) originating from one bidentate chelated

carboxylate, one oxygen atom (O9) afforded by one monodentate carboxylate, and three oxygen atoms (O6, O7 and O8) from three coordinated water molecules. The Zn—O bond distances vary from 0.195 0(4) to 0.232 7(4) nm. The  $\text{H}_4\text{L}$  in **1** are incompletely deprotonated ( $\text{H}_2\text{L}^{2-}$ ), exhibiting two different coordination modes, and there are only two carboxylate groups participating in the coordination with Zn(II) ions, as shown in Scheme 1. So, there are two different kinds of  $\text{H}_2\text{L}^{2-}$  ligands (namely,  $\text{H}_2\text{L}^{2-}$ -I and  $\text{H}_2\text{L}^{2-}$ -II). Two carboxylate groups of the first type ( $\text{H}_2\text{L}^{2-}$ -I) both adopts monodentate bridging modes (Mode I of Scheme 1), and there exist five torsion angles:  $169.601^\circ$ ,  $-76.517^\circ$ ,

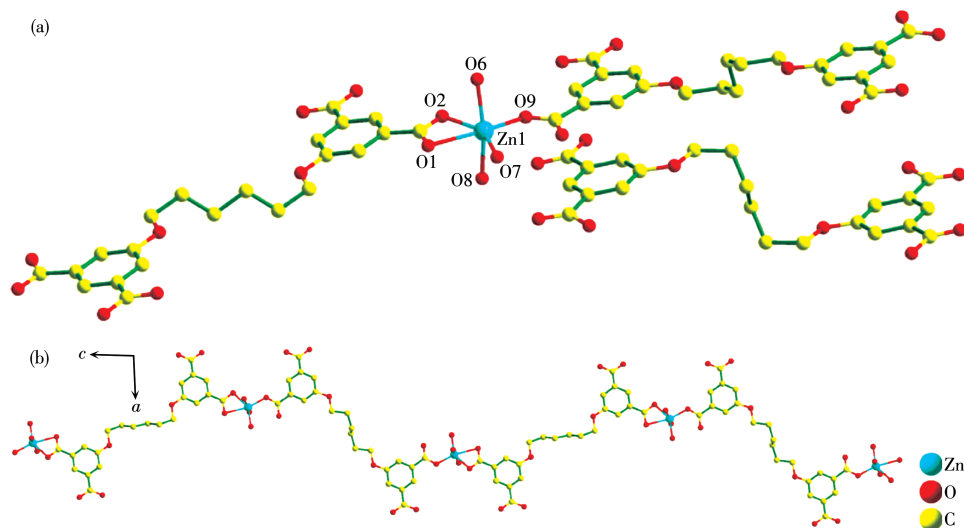
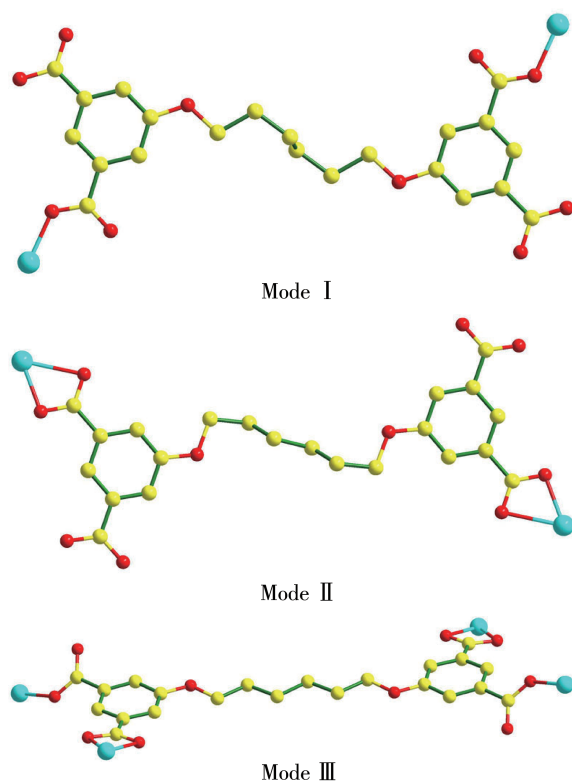


Fig.1 (a) Coordination environment of Zn(II) ion in **1** with hydrogen atoms omitted for clarity; (b) View of 1D infinite chain formed by  $\text{H}_2\text{L}^{2-}$  and Zn(II) ions

$-180.00^\circ$ ,  $76.517^\circ$  and  $169.601^\circ$ . The two carboxylate groups of the second type ( $\text{H}_2\text{L}^{2-}$ -II) both adopt bidentate chelating modes (Mode II of Scheme 1), and there exist five torsion angles of  $-60.766^\circ$ ,  $170.892^\circ$ ,  $180.000^\circ$ ,  $170.892^\circ$  and  $60.766^\circ$  in  $\text{H}_2\text{L}^{2-}$ -II. On the basis of the connection mode, each Zn(II) ion is joined by  $\text{H}_2\text{L}^{2-}$  anions into a 1D chain (Fig.1b).



Scheme 1 Schematic view of versatile coordination modes of  $\text{H}_2\text{L}^{2-}/\text{L}^{4-}$  ligand

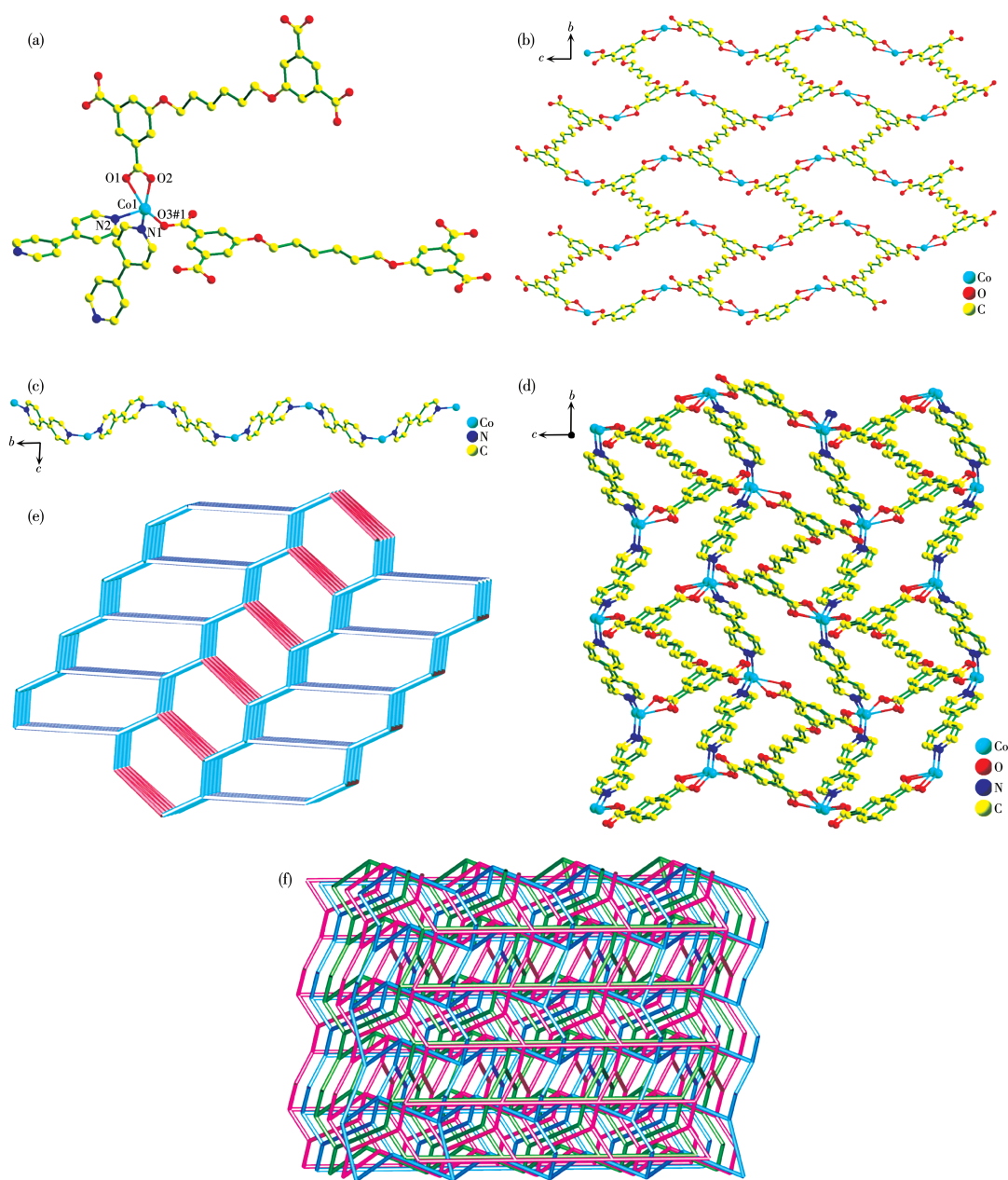
## 2.2 Crystal structure of $\{[\text{Co}(\text{L})_{0.5}(\text{4,4}'\text{-bpy})] \cdot 0.5\text{H}_2\text{O}\}_n$ (**2**)

When 4,4'-bpy was introduced into the reaction system, complex **2** was obtained. Single crystal X-ray diffraction analysis declares that **2** crystallizes in the monoclinic system with  $P2_1/c$  space group. As portrayed in Fig.2a, the structure of **2** contains one crystallographically unique Co(II) ion, half a  $\text{L}^{4-}$  ligand, one 4,4'-bpy ligand and half a water molecule. Each five-coordinated Co1 center is coordinated by three carboxylate oxygen atoms (O1, O2 and O3A) from two different  $\text{L}^{4-}$  ligands (Co1—O1 0.238 2(6) nm, Co1—O2 0.202 5(6) nm, Co1—O3A 0.199 7(6) nm) and two nitrogen donors (N1 and N2) from two distinct 4,4'-bpy

ligands (Co1—N1 0.207 2(6) nm, Co1—N2 0.210 8(6) nm). The bond angles around Co1 range from  $58.9(2)^\circ$  to  $157.6(2)^\circ$ . There is one kind of  $\text{L}^{4-}$  ligand in **2**, and there exist five torsion angles:  $176.737^\circ$ ,  $-179.920^\circ$ ,  $180.000^\circ$ ,  $179.920^\circ$  and  $-176.737^\circ$ . Two carboxylate groups of  $\text{L}^{4-}$  ligand adopt chelating bidentate modes, and the other two are in bridging monodentate modes (Mode III of Scheme 1). By this way, each Co(II) ion is joined by  $\text{L}^{4-}$  anions into a 2D net running along  $b$  and  $c$  axes (Fig.2b). The 1D infinite wave chain (Co(II)/4,4'-bpy chain) along the crystallographic  $a$ -axis is formed by the 4,4'-bpy spacers and Co(II) ions with a  $\text{Co}\cdots\text{Co}$  distance of 1.109 54 nm (Fig.2c). The Co(II)/ $\text{L}^{4-}$  nets are pillared by 1D chains of Co(II)/4,4'-bpy via the Co—N connections to produce a 3D framework (Fig.2d). Topologically, the Co cation can be clarified as a 4-connected node, which is connected to four equivalent nodes through two 4,4'-bpy ligands and two  $\text{L}^{4-}$  anions. Each  $\text{L}^{4-}$  anion links four Co(II) ions, so the  $\text{L}^{4-}$  is taken as a 4-connected node. Furthermore, the 4,4'-bpy is simplified as linear linkers. So, **2** represents a 3D topological net (Fig.2e) and the Schläfli symbol for **2** is  $(6^4 \cdot 7 \cdot 8)(6 \cdot 7^2)$ . Careful inspection of the structure of complex **2** suggests that it is a 3D 3-fold interpenetrating framework, as shown in Fig.2f.

## 2.3 Crystal structure of $\{[\text{Co}(\text{L})_{0.5}(\text{pbmb})(\text{H}_2\text{O})] \cdot \text{H}_2\text{O}\}_n$ (**3**)

The X-ray structural determination manifests that complex **3** is a 2D network. The asymmetric unit of **3** possesses one crystallographically independent Co(II) ion, half a  $\text{L}^{4-}$  ligand, one pbmb ligand, one coordinated water molecule and one lattice water molecule. In accordance with Fig.3a, Co1 ion is in a six-coordinated mode, in which Co1 is equatorially bonded to three carboxylic oxygen atoms (O1, O4A and O5A) from two different  $\text{L}^{4-}$  ligands (Co1—O1 0.204 89(16), Co1—O4A 0.219 60(17), Co1—O5A 0.214 59(18) nm) and one N atom from one pbmb ligand (Co1—N1 0.209 3(2) nm). The two axial sites on the metal are occupied by one N atom from one pbmb ligand (Co1—N3 0.216 0(2) nm) and one carboxyl O from one coordinated water molecule (Co1—O6 0.222 39(19) nm). The bond angles around Co(II) ions range from  $60.32(6)^\circ$  to  $176.68(7)^\circ$ .



Hydrogen atoms and solvent molecules are omitted for clarity; Symmetry code: #1:  $x, 3/2-y, -1/2+z$

Fig.2 (a) Coordination environment around the Co(II) centers in **2**; (b) 2D sheet structure constructed from Co(II) centers and parts of  $L^{4-}$  anions; (c) 1D infinite chain constructed by 4,4'-bpy and Co(II) ions along  $a$  axis; (d) Schematic view of 3D architecture of **2**; (e) Single 3D topology network; (f) Schematic representation of 3-fold interpenetrated topology nets for **2**

There are also one kind of  $L^{4-}$  ligand in **3**, and there exist five torsion angles:  $177.774^\circ$ ,  $-176.531^\circ$ ,  $180.000^\circ$ ,  $176.531^\circ$  and  $-177.774^\circ$ . Two carboxylate groups of  $L^{4-}$  ligand adopts chelating bidentate modes, and the other two are in bridging monodentate modes (Mode III of Scheme 1). By the coordination mode, the  $L^{4-}$  anion acts as a bridging ligand to bind the Co(II)

ions forming a 1D chains along  $b$  direction (Fig. 3b). The pbmb adopts asymmetrical *trans*-conformation with two different  $N_{\text{donor}} \cdots N - C_{sp^3} \cdots C_{sp^3}$  torsion angle of  $90.508^\circ$  and  $102.50^\circ$ . Co1 atom and symmetry-related Co atom are connected by two pbmb ligands forming a  $[\text{Co}(\text{pbmb})_2]$  unit with a 20-membered metallorings. The bridged  $\text{Co} \cdots \text{Co}$  distance along  $\mu$ -pbmb is  $0.99738$

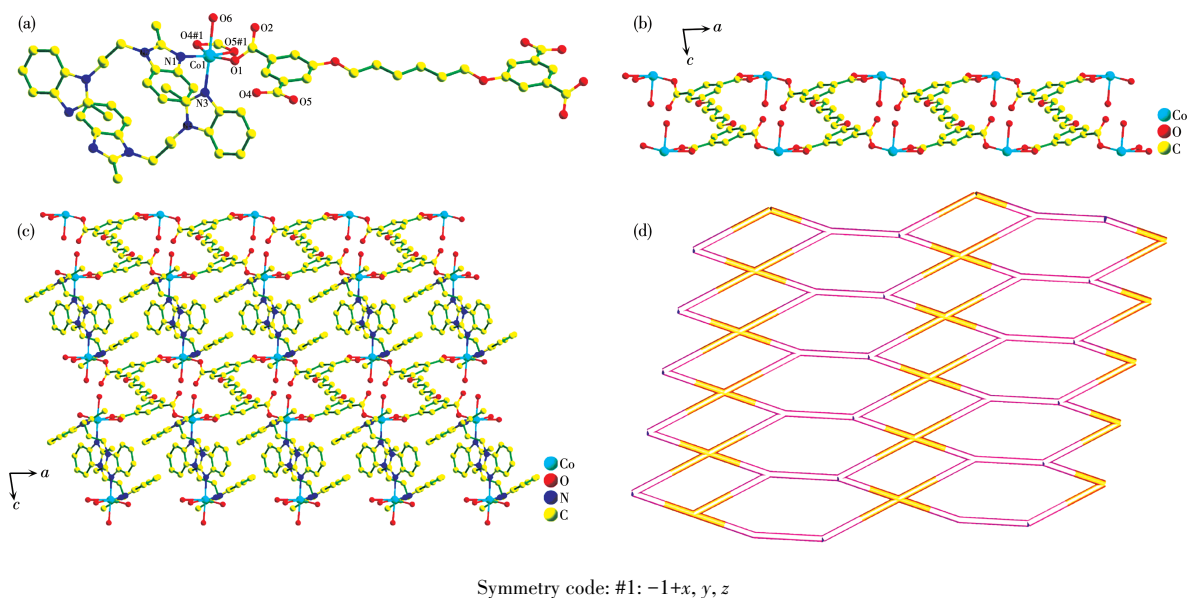


Fig.3 (a) Coordination environment of Co(II) ion in **3** with hydrogen atoms omitted for clarity; (b) 1D Co(II)/L<sup>4-</sup> chains; (c) 2D layer structure of **3**; (d) Schematic view of 2D topological network for **3** with point symbol of (4·6<sup>2</sup>)(4<sup>2</sup>·6<sup>2</sup>·8<sup>2</sup>)

nm. Two neighboring 1D Co(II)/L<sup>4-</sup> chains are connected together by sharing the metal ion from [Co(pbmb)]<sub>2</sub> unit, leading to the formation of the 2D layer of **3** along *a* and *c* axes (Fig.3c). Better insight into the 2D sheet can be fulfilled by topology analysis. Each Co(II) ion links two L<sup>4-</sup> and one [Co(pbmb)]<sub>2</sub> unit. As a consequence, the Co(II) ion is regarded as a 3-connector. While each L<sup>4-</sup> anion links four Co(II) ions, hence, the L<sup>4-</sup> can be known as a 4-connected linker. At last, the whole structure of **3** can be rationalized as a 2D topology network with the Schläfli symbol (4·6<sup>2</sup>)(4<sup>2</sup>·6<sup>2</sup>·8<sup>2</sup>) (Fig.3d).

#### 2.4 Effects of coordination modes of H<sub>2</sub>L<sup>2-</sup>/L<sup>4-</sup> anion and N-donor ligands on the frameworks of complexes **1**~**3**

On the basis of the descriptions above, we find that the H<sub>2</sub>L<sup>2-</sup>/L<sup>4-</sup> anion can adopt different coordination modes, linking to two (complexes **1**~**2**) or four (complex **3**) metal ions.

In **1**~**2**, each H<sub>2</sub>L<sup>2-</sup>/L<sup>4-</sup> anion all connects two Zn(II)/Co(II) ions corresponding to Mode I and II, severally (Scheme 1). Different from **1**~**2**, each L<sup>4-</sup> anion in **3** links with four Co(II) ions corresponding to Mode III (Scheme 1). The structural diversities of **1**~**3** can be attributed to the disparate coordination modes of carboxylate groups and the distinction of distortion degree

of flexible chain in the H<sub>4</sub>L molecule. For **1**, the carboxylate group of H<sub>2</sub>L<sup>2-</sup> anion bind with the central metals in a (κ<sup>1</sup>)-(κ<sup>1</sup>)-μ<sub>2</sub> fashion and (κ<sup>2</sup>)-(κ<sup>2</sup>)-μ<sub>2</sub> fashion. This kind of coordination fashion in **1** leads to the formation of 1D Zn(II)/H<sub>2</sub>L<sup>2-</sup> chain. For **2** and **3**, the carboxylate group of L<sup>4-</sup> anion coordinate with the central metals in a (κ<sup>1</sup>)-(κ<sup>2</sup>)-(κ<sup>1</sup>)-(κ<sup>2</sup>)-μ<sub>4</sub> fashion. This type of coordination fashion in **2** gives rise to the presence of 2D Co(II)/L<sup>4-</sup> net; while that in **3** brings about the generation of 1D Co(II)/L<sup>4-</sup> double chain.

The N-donor ligands have a profound influence on the resultant structures of the complexes. The 4,4'-bpy in **2** bridge Co(II) ions to yield a 1D chain of Co(II)/4,4'-bpy. The Co(II)/4,4'-bpy chain serves as pillars, linking the neighbouring Co(II)/L<sup>4-</sup> nets into a 3-fold interpenetrated 3D framework with a vertex symbol of (4·6<sup>2</sup>)(4<sup>2</sup>·6<sup>2</sup>·8<sup>2</sup>). In **3**, asymmetrical *trans*-conformational pbmb ligand coordinates with Co1 atom and symmetry-related Co atom giving rise to a [Co(pbmb)]<sub>2</sub> unit with a 20-membered metallorings. The combination of the 1D Co(II)/L<sup>4-</sup> chain and [Co(pbmb)]<sub>2</sub> unit leads to a 2D net with point symbol of (6<sup>6</sup>)<sub>2</sub>(6<sup>4</sup>·8<sup>2</sup>).

#### 2.5 Thermal analyses

The thermal stability of complexes **2**~**3** were also estimated (Fig.4). For **2**, the TGA shows that the first weight loss of 2.14% in a range of 117~163 °C is relat-

ed to the loss of half a lattice water molecule (Calcd. 2.02%). The overall framework of **2** began to decompose from 224 °C, corresponding to the losses of  $L^{4-}$  and 4,4'-bpy, and the CoO residue of 16.54% (Calcd. 16.82%) was observed at 494 °C. For **3**, the TGA shows that the first weight loss of 6.28% in a range of 114~151 °C is related to the loss of one coordinated water molecule and one lattice water molecule (Calcd. 5.80%). The overall framework of **3** began to decompose from 292 °C, corresponding to the losses of  $L^{4-}$  and pbmb, and the CoO residue of 12.03% (Calcd. 12.07%) was observed at 472 °C.

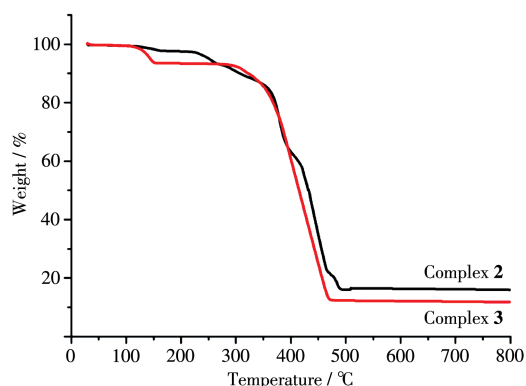


Fig.4 TG curves of complexes **2** and **3**

## 2.6 Photoluminescence properties

Photoluminescence properties of the complexes with  $d^{10}$  metal centers have aroused great interest owing to their latent applications<sup>[14-18]</sup>. Hence, the photoluminescent spectra of the free  $H_4L$  ligand and complex **1** were investigated at room temperature (Fig. 5). The spectrum of free ligand  $H_4L$  displayed an emission band at 429 nm ( $\lambda_{ex}$  = 330 nm). The spectrum of com-

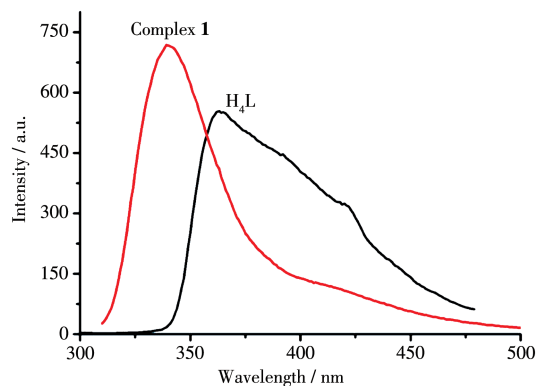


Fig.5 Photoluminescent spectra of free  $H_4L$  ligand and complex **1**

plex **1** exhibited the emission maxima at 339 nm ( $\lambda_{ex}$  = 277 nm). As compared to the  $H_4L$  ligand, a hypsochromic shift (90 nm) was observed. The emission spectrum of **1** was parallel to that of  $H_4L$  ligand, which also be mainly attributed to the intraligand emission of  $H_4L$ <sup>[19]</sup>.

## 3 Conclusions

In brief, three Zn(II)/Co(II) complexes have been prepared under solvo-/hydrothermal conditions, by using  $H_4L$  with the introduction of rationally selected 4, 4'-bpy and pbmb ancillary ligands. Complex **1** is 1D chain structure. Complex **2** is 3D framework. Complex **3** is 2D network. Besides, **1** showed fluorescence properties.

## References:

- [1] Yang X G, Ma L F, Yan D P. *Chem. Sci.*, **2019**,**10**:4567-4572
- [2] Wu Y P, Tian J W, Liu S, Li B, Zhao J, Ma L F, Li D S. *Angew. Chem. Int. Ed.*, **2019**,**58**:12185-12189
- [3] Fu H R, Wang N, Qin J H, Han M L, Ma L F, Wang F. *Chem. Commun.*, **2018**,**54**:11645-11648
- [4] Li Y, Mo Z W, Zhang X W, Zheng K, Zhou D D, Zhang J P. *Cryst. Growth Des.*, **2020**,**20**:7021-7026
- [5] Zhou H C, Kitagawa S. *Chem. Soc. Rev.*, **2014**,**43**:5415-5418
- [6] Liu W L, Yu J H, Jiang J X, Yuan L M, Xu B, Liu Q, Qu B T, Zhang G Q, Yan C G. *CrystEngComm*, **2011**,**13**:2764-2773
- [7] Zhang X P, Zhou J M, Shi W, Zhang Z J, Cheng P. *CrystEngComm*, **2013**,**15**:9738-9744
- [8] Ghosh S K, Bharadwaj P K. *Inorg. Chem.*, **2004**,**43**:5180-5182
- [9] Zhang J, Chen Y B, Chen S M, Li Z J, Cheng J K, Yao Y G. *Inorg. Chem.*, **2006**,**45**:3161-3163
- [10] Eddaoudi M, Moler D B, Li H, Chen B L, Reineke T M, O'Keeffe M, Yaghi O M. *Acc. Chem. Res.*, **2001**,**34**:319-330
- [11] Bronisz R. *Inorg. Chem.*, **2005**,**44**:4463-4465
- [12] Sheldrick G M. *Acta Crystallogr. Sect. A*, **2008**,**A64**:112-122
- [13] Dolomanov O V, Bourhis L J, Gildea R J, Howard J A K, Puschmann H. *J. Appl. Cryst.*, **2009**,**42**:339-341
- [14] Yahsi Y, Ozbek H, Aygun M, Kara H. *Acta Crystallogr. Sect. C*, **2016**,**C72**:426-431
- [15] Tsai C W, Kroon R E, Swart H C, Terblans J J, Harris R A. *J. Lumin.*, **2019**,**207**:454-459
- [16] Han Y, Li H J, Li Y Y, Sun J, Sun Y X, Sun L W, Wang H L, Wang L. *Inorg. Chim. Acta*, **2017**,**467**:136-146
- [17] Bai H Y, Ma J F, Yang J, Liu Y Y, Wu H, Ma J C. *Cryst. Growth Des.*, **2010**,**10**:995-1016
- [18] Odabaşıoğlu S, Kurtaran R, Azizoglu A, Kara H, Oz S, Atakol O. *Cent. Eur. J. Chem.*, **2009**,**7**(3):402-409
- [19] Fang S M, Chen M, Yang X G, Wang C, Du M, Liu C S. *CrystEngComm*, **2012**,**14**:5299-5304